This document is downloaded from DR-NTU, Nanyang Technological University Library, Singapore.

Title	Detection of Ge and Si intermixing in Ge/Si using multiwavelength micro-raman spectroscopy
Author(s)	Yoo, Woo Sik; Kang, Kitaek; Ueda, Takeshi; Ishigaki, Toshikazu; Nishigaki, Hiroshi; Hasuike, Noriyuki; Harima, Hiroshi; Yoshimoto, Masahiro; Tan, Chuan Seng
Citation	Yoo, W. S., Kang, K., Ueda, T., Ishigaki, T., Nishigaki, H., Hasuike, N., et al. (2014). Detection of Ge and Si Intermixing in Ge/Si Using Multiwavelength Micro-Raman Spectroscopy. ECS Transactions, 64(6), 79-88.
Date	2014
URL	http://hdl.handle.net/10220/25012
Rights	© 2014 The Electrochemical Society. This paper was published in ECS Transactions and is made available as an electronic reprint (preprint) with permission of The Electrochemical Society. The paper can be found at the following official DOI: [http://dx.doi.org/10.1149/06406.0079ecst]. One print or electronic copy may be made for personal use only. Systematic or multiple reproduction, distribution to multiple locations via electronic or other means, duplication of any material in this paper for a fee or for commercial purposes, or modification of the content of the paper is prohibited and is subject to penalties under law.

ECS Transactions, 64 (6) 79-88 (2014)
10.1149/06406.0079ecst ©The Electrochemical Society

Detection of Ge and Si Intermixing in Ge/Si using Multiwavelength Micro-Raman Spectroscopy

Woo Sik Yoo[a], Kitaek Kang[a], Takeshi Ueda[a], Toshikazu Ishigaki[a], Hiroshi Nishigaki[b], Noriyuki Hasuike[b], Hiroshi Harima[b], Masahiro Yoshimoto[b], and Chuan Seng Tan[c]

[a] WaferMasters, Inc., San Jose, California 95112, USA
[b] Kyoto Institute of Technology, Kyoto, 606-8585, Japan
[c] Nanyang Technological University, Singapore, 639798, Singapore

To meet various physical property requirements of materials for advanced application, for specific devices, combinations of Si/Ge, Ge/Si, $Si_{1-x}Ge_x$/Si, are frequently introduced in the device fabrication process. Epitaxy, condensation and annealing processes are commonly used. Since a small variation in composition, strain and crystallinity can result in reduced device performance or failure, the composition, strain and crystallinity must be carefully monitored and controlled throughout the manufacturing process. We report the detection of Ge and Si intermixing in epitaxially grown Ge/Si after successive thermal anneals using multiwavelength Raman spectroscopy. We have studied the dependence of Ge and Si intermixing on annealing temperature and Raman excitation wavelength. Very strong dependence of signal-to-noise (S/N) ratio measurements on excitation wavelength and film structure was observed. Suitable excitation wavelengths must be chosen to properly detect and characterize Si and Ge intermixing, based on the stacking order of epitaxial films and thicknesses.

Introduction

As a natural way to extend the lifespan of Si in fast and highly functional devices, integration of hetero-components such as Ge, or alloys of Ge with Si, has been widely pursued. Ge has very promising electronic properties: 2.75 times higher electron mobility (3900 $cm^2/V{\cdot}sec$), 4.0 times higher hole mobility (1900 $cm^2/V{\cdot}sec$) and one half the bandgap energy (0.67eV) at room temperature as compared to Si (1, 2). Ge has a lattice constant 4.2% larger than that of Si while they have the same crystalline structure (face centered cubic (fcc), diamond structure). The smaller bandgap of Ge, compared with Si, enabled the bandgap engineering of heterostructures for very fast and high frequency operating devices. The 4.2% lattice mismatch between Ge and Si makes continuous high quality and smooth film growth difficult. Ge island formation takes place beyond the critical thickness of a few atomic layers (3, 4). To solve lattice mismatch originated heteroepitaxial problems, various techniques such as the growth of graded buffer layers and/or surfactant mediated epitaxy have been successfully implemented (5-9).

To meet various physical property requirements of materials for advanced application, specific devices, combinations of Si/Ge, Ge/Si, $Si_{1-x}Ge_x$/Si are frequently introduced. Potential applications of hetero-epitaxial Ge technology are Ge complimentary metal-oxide-semiconductor (CMOS) for high performance devices, short wave infrared (SWIR)

Downloaded on 2015-02-01 to IP 155.69.4.4 address. Redistribution subject to ECS terms of use (see ecsdl.org/site/terms_use) unless CC License in place (see abstract).

Ge photodetector for Si-based optoelectronic devices, and integrated Ge/Si (Ge p-MOS and Si n-MOS) devices (10-12). Epitaxy, condensation and annealing processes are commonly used for fabricating these heterostructures (5-9, 13, 14). Because a small variation in composition, strain, profile and crystallinity can result in reduced device performance or failure, the composition, strain and crystallinity must be carefully monitored and controlled throughout the manufacturing process.

In this paper, we have characterized as-grown heteroepitaxial Ge/Si wafers and annealed heteroepitaxial Ge/Si wafers using multiwavelength Raman spectroscopy for noncontact, composition depth profiling.

Experiment

Approximately 1 μm thick Ge films were epitaxially grown on p-Si (100) wafers with resistivity ranging from 4 ~ 10 Ω·cm in a commercially available chemical vapor deposition (CVD) reactor operating in the temperature range of 550 ~ 700°C. Details of Ge epitaxial growth on Si are published elsewhere (15). Due to the large (4.2%) lattice mismatch between Ge and Si, the epitaxial Ge films typically have high density threading dislocations (TD) at the Ge/Si interface. For 1 μm thick epitaxial Ge film on Si, the threading dislocation density (TDD) is as high as 10^8 cm^{-2} (16). The TDD tends to decrease as the epitaxial Ge film grows and it becomes an order of magnitude smaller in 2 μm thick epitaxial Ge on Si. The TDD also decreases after a few minutes of thermal annealing (or cycling) above the epitaxial growth temperature (16-19).

Selected epitaxial Ge/Si wafers were annealed in the temperature range of 800 ~ 875°C for 3 min to investigate the effects of thermal annealing (cycling) on possible changes in composition (intermixing of Ge and Si) during typical TDD reduction annealing conditions.

On the selected as-grown heteroepitaxial Ge/Si wafers, most of the (0.8 μm) epitaxial Ge films were removed by chemical mechanical polishing (CMP) to investigate the composition and the possibility of Ge-Si intermixing near the Ge/Si interface. The final epitaxial Ge layer thickness was reduced to ~ 0.2 μm after CMP.

All heteroepitaxial Ge/Si wafers were examined by multiwavelength Raman spectroscopy in the wavenumber range of 250 ~ 600 cm^{-1} before and after annealing and/or CMP. For different wavelengths of 457.9, 488.0, 514.5 and 785 nm laser lines with different probing depths were used as the Raman excitation source. Raman measurement was performed in a backscattering mode. The excitation laser beam was irradiated from the epitaxial Ge film side through a microscope objective lens. The diameter of the excitation laser beam on the wafer surface was approximately 1 μm. Effective Raman excitation wavelengths for various Ge/Si and possible alloy structures of Ge with Si were investigated.

Results and Discussions

Figure 1 shows 514.5 nm excited linear and log scale Raman spectra from reference Si, reference Ge, reference thin (0.2 μm thick) epitaxial Ge/Si and epitaxially grown 1.0 μm thick Ge/Si wafers after thermal annealing in the temperature range of 800 ~ 875°C. The annealing time was fixed at 3 min for all epitaxial Ge/Si wafers.

Ge and Si show a very sharp Raman peak at 300 cm^{-1} and 520.3 cm^{-1}, respectively. The peak position shifts under the presence of strain/stress and isotopic variations (4, 20-

Downloaded on 2015-02-01 to IP 155.69.4.4 address. Redistribution subject to ECS terms of use (see ecsdl.org/site/terms_use) unless CC License in place (see abstract).

22). Alloys of Si and Ge ($Si_{1-x}Ge_x$) typically show three Raman peaks of Ge-Ge (~300 cm^{-1}), Si-Ge (~400 cm^{-1}) and Si-Si (~500 cm^{-1}). The position and intensity of the three peaks depend on the composition of the alloys. The alloy composition can be estimated from Raman spectra (position and intensity ratios of the three peaks) (23-25). The presence of Ge and Si intermixing can easily be determined by searching for the Si-Ge peak at ~400 cm^{-1}.

The linear plot of the Raman spectra (Fig. 1 (a)) only showed a Ge peak ~ 300 cm^{-1} and Si peak around ~520 cm^{-1}. No Si-Ge peak near ~400 cm^{-1} from $Si_{1-x}Ge_x$ alloy was recognized. The Ge reference wafer and 1 µm thick epitaxial Ge/Si wafers annealed below 850°C showed a single Ge peak at ~300 cm^{-1} implying the wafer surface is pure Ge within the probing depth of 514.5 nm excitation wavelength. The thin (0.2 µm thick) Ge/Si reference wafer showed two peaks (one strong Ge peak at ~300 cm^{-1} and one weak Si peak at ~520 cm^{-1}). There is no Si-Ge peak near ~400 cm^{-1} from a $Si_{1-x}Ge_x$ alloy from the thin (0.2 µm thick) Ge/Si reference wafer. The 1 µm thick epitaxial Ge/Si wafers annealed at 850°C showed one very weak Ge peak at ~300 cm^{-1} and a strong Si peak at ~520 cm^{-1}. The Si reference wafer and 1 µm thick epitaxial Ge/Si wafers annealed at 875°C showed one strong Si peak at ~520 cm^{-1}. The Ge peak at ~300 cm^{-1} completely disappeared from the 1 µm thick epitaxial Ge/Si wafers annealed at 875°C. No sign of $Si_{1-x}Ge_x$ alloy formation was observed from the linear plot Raman spectra. To investigate the disappearance of the Ge peak and possible change of the epitaxial layer composition after high temperature thermal annealing, the Raman spectra were re-plotted in log scale (Fig. 1 (b)).

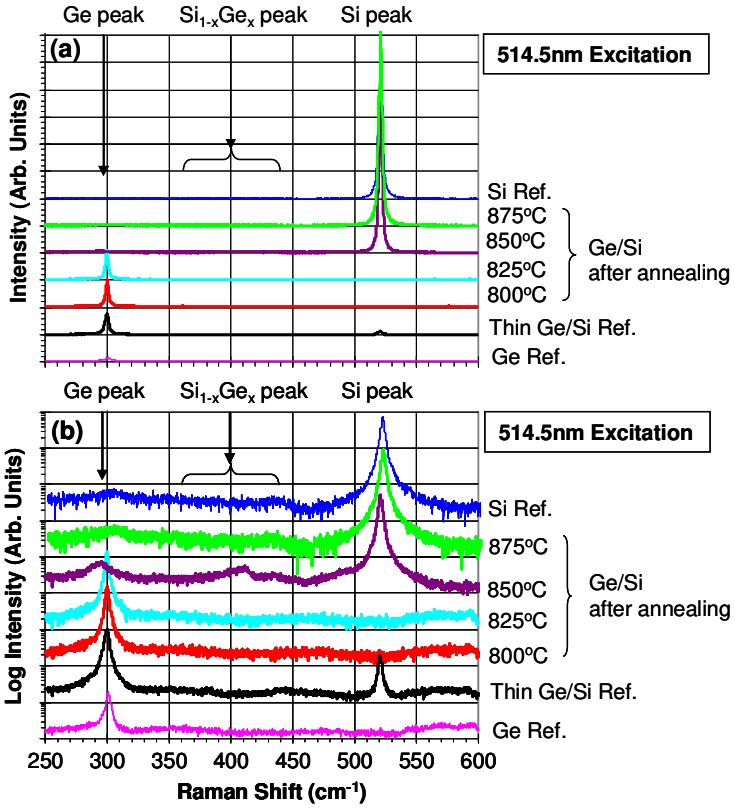

Figure 1. Linear and log scale Raman spectra from 1.0 µm thick epitaxial Ge/Si wafers after thermal annealing in the range of 800 ~ 875°C. Raman spectra from Si, thin (0.2 µm thick) epitaxial Ge/Si and Ge wafers were also shown as references. (Excitation wavelength: 514.5 nm)

Downloaded on 2015-02-01 to IP 155.69.4.4 address. Redistribution subject to ECS terms of use (see ecsdl.org/site/terms_use) unless CC License in place (see abstract).

The log plot of Raman spectra (Fig. 1 (b)) showed little detail of the very weak Raman peaks. Ge peak ~ 300 cm^{-1}, Si-Ge peak ~400 cm^{-1}, Si peak around ~520 cm^{-1} and broad background corresponding to phonon density of states (DOS) of Si in the wavenumber range of 250 ~ 450 cm^{-1} were found. Similar to the linear plot of Raman spectra, the Ge reference wafer and 1 μm thick epitaxial Ge/Si wafers annealed below 850°C only showed a single Ge peak at ~300 cm^{-1} implying the wafer surface is pure Ge. However, the 1 μm thick epitaxial Ge/Si wafer annealed below 850°C showed a Ge peak at ~300 cm^{-1}, a Si peak at ~520 cm^{-1} and a distinct peak ~410 cm^{-1} corresponding to Si-Ge alloy. It indicates Si-Ge alloy formation during annealing at 850°C. Both the Ge peak at ~300 cm^{-1} and Si peak at ~520 cm^{-1} were slightly shifted downwards from pure Ge and pure Si peaks due to the Si-Ge alloy formation. The 1 μm thick epitaxial Ge/Si wafer annealed at 875°C showed almost identical Raman spectra with broad background peaks related to the phonon DOS from the reference Si wafer. The Ge atoms may have diffused into the Si wafer and average Ge concentration may have become very low after 875°C annealing so that no Si-Ge and Ge related Raman peaks were observed, even from the Raman spectra plotted in the log scale. When either Ge or Si content is less than 5 atomic percent (at. %) in thin heteroepitaxial films on foreign wafers (such $Si_{>0.95}Ge_{<0.05}$/Si or $Si_{<0.05}Ge_{>0.95}$/Ge), it is difficult to distinguish the Raman peak from the Si-Ge alloy films from the Raman peak from the wafer. This is because the Raman peak from the Si-Ge alloy becomes very weak and overlaps with the Raman peak from the wafer. A log scale plot of Raman spectra can be more effective in detecting Si-Ge alloy formation when the Si-Ge related Raman peak ~400 cm^{-1} is very weak or unrecognizable.

It is well known that the probing depth of Raman measurements depends on excitation wavelength and optical properties of the specimen. The optical properties of a specimen can vary over a wide range depending on materials, thickness, number of layers, stacking order, presence of patterns etc. The excitation wavelength of Raman measurements must be carefully chosen after considering various factors listed above. To investigate the effect of Raman excitation wavelengths on the detection capability of Si and Ge intermixing (or alloy formation), Raman spectra from the same set of reference wafers and Ge/Si wafers were measured under three excitation wavelengths of 457.9, 488.0 and 514.5 nm. For sensitive detection of Si-Ge alloy formation, all Raman spectra were plotted in log scale (Fig. 2).

The Raman spectra from the same set of reference and epitaxial Ge/Si wafers under three different excitation wavelengths look very similar. The 488.0 nm excited Raman spectra generally showed noisier results (low signal-to-noise (S/N) ratio) even though the overall intensity of Raman peaks of Ge and Si are stronger than those measured under 457.9 and 514.5 nm excitation. As the excitation wavelength is shorter, the Ge-Ge peak near ~300 cm^{-1}, Si-Ge peak near ~400 cm^{-1} and Si-Si peak near ~500 cm^{-1} from the $Si_{1-x}Ge_x$ (Si-Ge alloy) layer of 1 μm thick epitaxial Ge/Si wafer, annealed at 850°C, became clearer. Based on the Si-Si peak position at ~490 cm^{-1} in Fig. 2 (a), the Ge content in $Si_{1-x}Ge_x$ (Si-Ge alloy) layer is estimated to be ~ 30 at. % ($x \approx 0.30$).

Under the same spectrometer configuration, Raman spectral resolution is higher at longer excitation wavelengths due to the higher dispersion at longer wavelengths. Detailed Raman spectra are generally expected from the longer wavelength excited Raman measurements from the specimen with a Si-Ge alloy with uniform Ge composition in the depth direction. Raman spectra from the 1 μm thick epitaxial Ge/Si wafer, annealed at 850°C, showed completely opposite trends. This suggests that the Ge content (x value) in the $Si_{1-x}Ge_x$ layer formed by thermal annealing at 850°C is not

Downloaded on 2015-02-01 to IP 155.69.4.4 address. Redistribution subject to ECS terms of use (see ecsdl.org/site/terms_use) unless CC License in place (see abstract).

uniform throughout the Si-Ge alloy layer (in the depth direction). Since the Si-Ge alloy layer is formed by thermal diffusion of Si and Ge atoms, a Ge content gradient in the Si-Ge alloy layer is easily expected. The detection of Si-Ge alloy formation (Ge/Si intermixing) within the probing depth of Raman excitation wavelength can be done at any excitation wavelength. However, multiwavelength excited Raman measurements are essential to detect the Ge content gradient in the Si-Ge alloy layer.

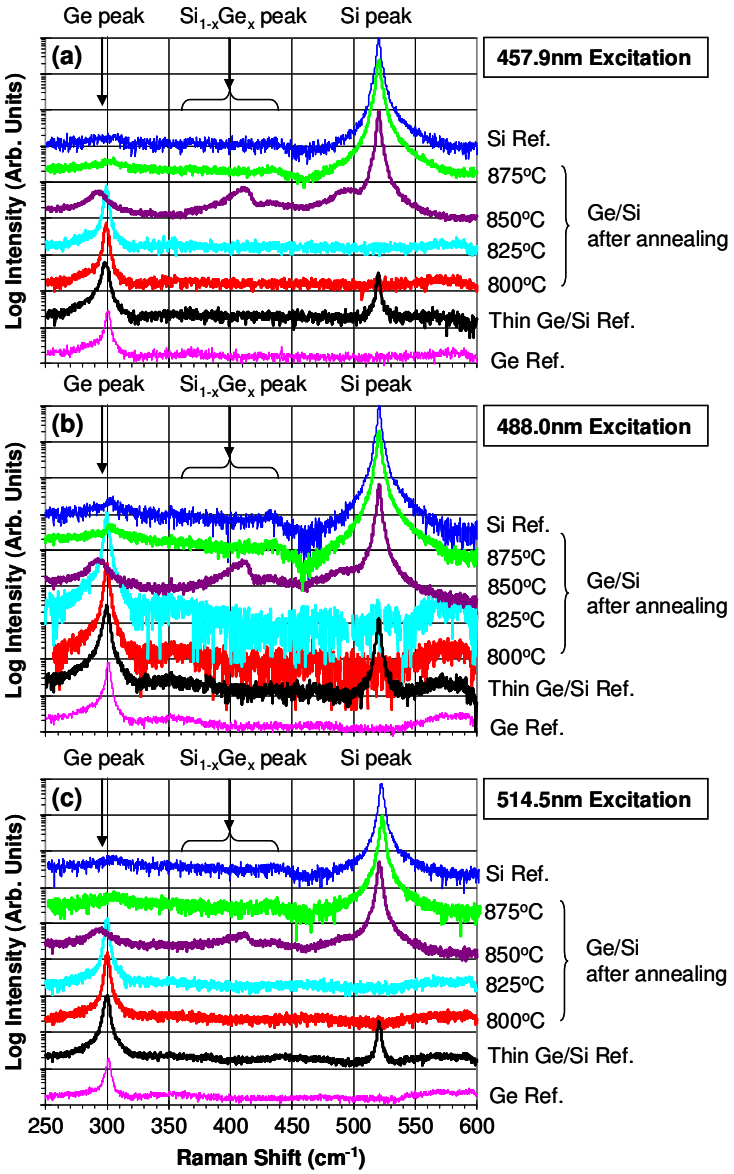

Figure 2. Log scale Raman spectra from 1.0 μm thick epitaxial Ge/Si wafers after thermal annealing in the temperature range of 800 ~ 875°C. Raman spectra from Si, thin (0.2 μm thick) epitaxial Ge/Si and Ge wafers were also shown as references. (Excitation wavelengths: 457.9, 488.0 and 514.5 nm)

It is important to understand the probing depth of Raman excitation wavelengths in Si, Ge and Si-Ge alloys. Optical properties of Si and Ge must be considered to properly select optimal Raman excitation wavelengths. Figure 3 shows (a) absorption coefficient,

Downloaded on 2015-02-01 to IP 155.69.4.4 address. Redistribution subject to ECS terms of use (see ecsdl.org/site/terms_use) unless CC License in place (see abstract).

(b) transmittance and (c) room temperature photoluminescence (PL) spectra of Si and Ge in the wavelength range of 0.2 μm and 3.0 μm.

The bandgap (Eg) values of Si and Ge are 1.12 and 0.67 eV, respectively. The light absorption edges (absorption coefficient (α) of 10^2 cm^{-1}) of Si and Ge are located at ~1.0 and ~1.6 μm. Si is ~56% transparent at wavelengths longer than 1.05 μm and Ge is ~44% transparent at wavelengths longer than 1.75 μm. The bandgap and optical properties of Si-Ge alloys ($Si_{1-x}Ge_x$) lie between those of Si and Ge. As the Ge content (x) increases, the bandgap and optical properties of $Si_{1-x}Ge_x$ depart from the Si properties and approach the Ge properties.

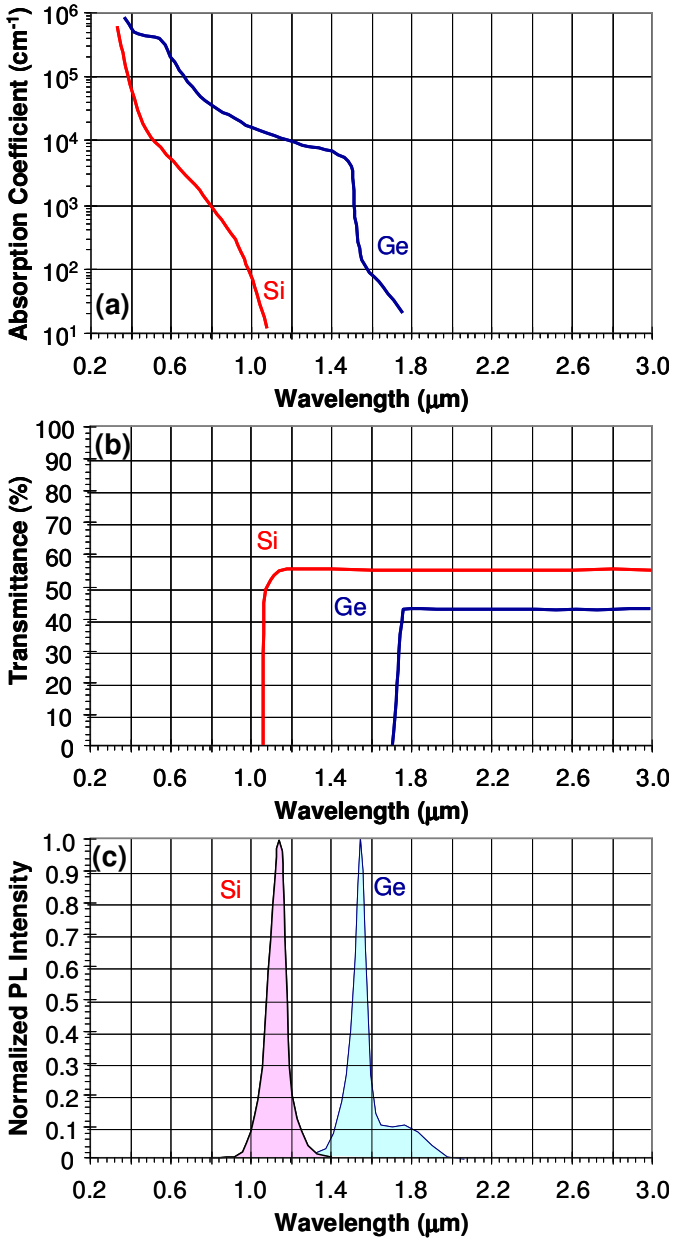

Figure 3. (a) absorption coefficient, (b) transmittance and (c) room temperature PL spectra of Si and Ge in the wavelength range of 0.2 μm and 3.0 μm.

Downloaded on 2015-02-01 to IP 155.69.4.4 address. Redistribution subject to ECS terms of use (see ecsdl.org/site/terms_use) unless CC License in place (see abstract).

When a highly transparent (low absorbing) film is on the measurement (Raman excitation) side (i.e. Si/Ge and $Si_{1-x}Ge_x$/Ge), shorter excitation wavelength Raman measurements can probe both film and substrate materials. In the opposite configuration, with a highly opaque (or absorptive) film on the Raman measurement side (i.e. Ge/Si and $Si_{1-x}Ge_x$/Si), the most likely Raman signals from the film are measured at many excitation wavelengths. Longer excitation wavelengths, with deeper probing depths, are highly desirable for investigating the interfaces of Ge/Si and $Si_{1-x}Ge_x$/Si heterostructures.

One other important consideration in selecting a proper Raman excitation wavelength is the luminescence or fluorescence bands (in this case, room temperature PL bands for Si, $Si_{1-x}Ge_x$ and Ge). Raman scattering yield of semiconductor crystals is typically on the order of parts per million (ppm) or less (26), while PL yields can easily be on the order of percent (%), even for the indirect semiconductors such as Si and Ge. When there is a PL signal from either film or substrate, the Raman signal from the specimen cannot be measured or separated. Typical room temperature PL spectra from Si and Ge are measured in the wavelength ranges of 850 ~ 1400 nm and 1200 ~ 2000 nm (Fig. 3 (c)) (27, 28). The Raman excitation wavelength must not be longer than 850 nm in the case of a Ge/Si, $Si_{1-x}Ge_x$/Ge or Si/Ge structure.

Absorption coefficients and corresponding Raman probing depths of Ge and Si, under various excitation wavelengths, are summarized in Table I. The absorption coefficient of Ge is at least one order of magnitude larger than that of Si for all excitation wavelengths (29, 30). The Raman probing depth for Ge is almost constant at 8 ~ 9 nm, up to 532 nm excitation, while the Raman probing depth for Si increases as the excitation wavelength is increased. In the case of ultra thin epitaxial $Si_{1-x}Ge_x$/Si, ultraviolet (UV) and/or near UV visible excitation wavelengths are frequently used (25).

TABLE I. Absorption coefficients and corresponding Raman probing depths of Ge and Si under various excitation wavelengths.

Excitation Wavelength (nm)	Absorption Coefficient α (cm^{-1})		Raman Probing Depth $\frac{1}{2}\delta_p$ (nm)	
	Ge	Si	Ge	Si
457.9	$6.13x10^5$	$3.55x10^4$	~8	~141
488.0	$6.06x10^5$	$2.03x10^4$	~8	~246
514.5	$5.97x10^5$	$1.46x10^4$	~8	~340
532	$5.77x10^5$	$1.02x10^4$	~9	~490
650	$1.00x10^5$	$3.08x10^3$	~50	~1623
785	$5.59x10^4$	$1.12x10^3$	~89	~4460
827	$4.53x10^4$	$7.60x10^2$	~110	~6578

The similarity of multiwavelength Raman spectra shown in Fig. 2 (a) ~ (c) can be explained by the constant probing depth of ~ 8 nm in Ge film under 457.9, 488.0 and 514.5 nm excitation. To effectively detect Ge/Si intermixing in epitaxial Ge/Si with Ge film thickness greater than 50 nm, the Raman excitation wavelength must be longer than 650 nm and shorter than 850 nm (to avoid interference from PL signal from Si). It is not easy to detect Ge/Si intermixing near the Ge/Si interface, if the Ge film thickness is in the range of microns, due to the high absorption coefficient of Ge. Any Si contamination and/or Ge/Si intermixing near the surface of Ge/Si can easily be detected under all excitation wavelengths listed in the Table I.

To prove the effectiveness of Raman measurements in detecting Si contamination and/or Ge/Si intermixing in epitaxial Ge/Si, an as-grown 1 μm thick Ge/Si wafer was characterized under for different excitation wavelengths (457.9, 488.0, 514.5 and 785 nm). The same specimen was measured after removing ~ 0.8 μm of Ge epitaxial layer by

Downloaded on 2015-02-01 to IP 155.69.4.4 address. Redistribution subject to ECS terms of use (see ecsdl.org/site/terms_use) unless CC License in place (see abstract).

CMP. The remaining epitaxial film thickness was ~ 0.2 µm. Figure 4 shows a linear scale Raman spectra from (a) as-grown 1 µm thick epitaxial Ge/Si wafer and (b) after CMP under four different excitation wavelengths.

No evidence of Si contamination and/or Ge/Si intermixing was found from the as-grown 1 µm thick Ge/Si wafer within the probing depths (~267 nm, 3 times the probing depth of 785 nm excitation, where >90% of Raman signal is originated) of all four excitation wavelengths. The ~0.2 µm thick Ge/Si wafer (after ~ 0.8 µm epitaxial Ge film removal by CMP) showed significant Ge/Si intermixing and Si-Ge alloy formation within the probing depths from the surface (8 nm ~ 89 nm) for all four excitation wavelengths after CMP. Since no Si Raman peak at ~520 cm^{-1} was measured, even under 785 nm excitation, we may assume the excitation light did not reach the Si wafer, approximately 0.2 µm below the surface, after the CMP. The Raman intensity increase and upward shift of Ge-Ge peak ~300 cm^{-1} and Si-Ge peak ~ 400 cm^{-1}, with excitation wavelength increase, strongly indicates the increase of probing volume and decrease of Ge content in the Si-Ge alloy layer towards the Ge/Si interface.

The intermixing of selectively grown Si dots with Ge core after 5 minutes of annealing at 800°C has been reported (31). Thermal inter-diffusion of Ge and Si in $Si_{1-x}Ge_x$/Si after 60s rapid thermal annealing (RTA) as low as 950°C has been reported (32). For successful integration of heterostructures of Si and Ge, very careful process monitoring and control are required to avoid surprising deviations in composition, profile and crystallinity from the designed specifications.

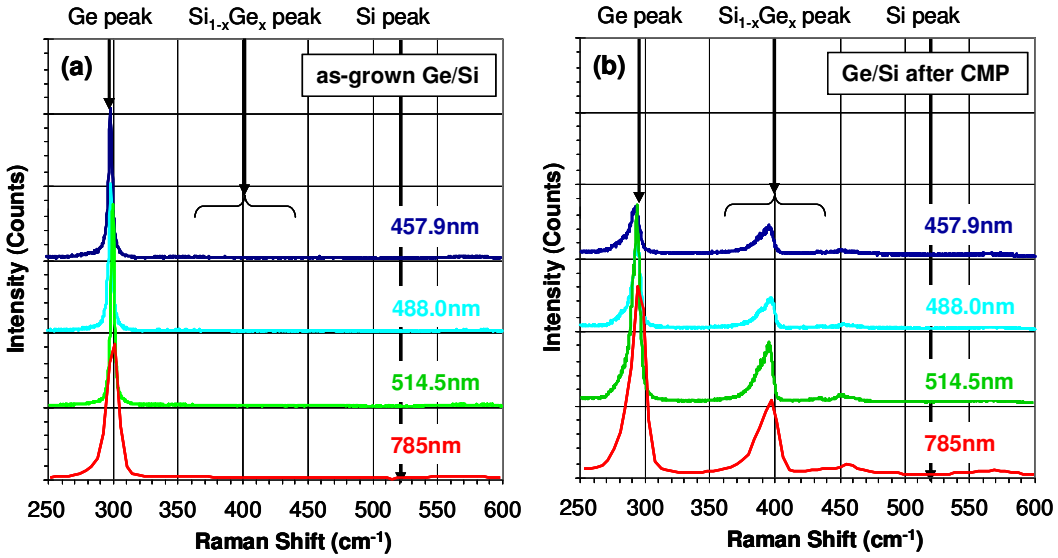

Figure 4. Linear scale Raman spectra from (a) as-grown 1 µm thick epitaxial Ge/Si wafer and (b) after CMP under four different excitation wavelengths (457.9, 488.0, 514.5 and 785 nm). Final Ge film thickness after CMP is 0.2 µm.

Multiwavelength Raman characterization techniques are very effective in detecting Si contamination and/or Ge/Si intermixing in epitaxial Ge/Si wafers. The effectiveness of Raman characterization and detection sensitivity of Si contamination, and/or Ge/Si intermixing in epitaxial Ge/Si wafers, for inline process monitoring can be significantly enhanced by selecting proper excitation wavelengths considering the material and structure of specimens.

Downloaded on 2015-02-01 to IP 155.69.4.4 address. Redistribution subject to ECS terms of use (see ecsdl.org/site/terms_use) unless CC License in place (see abstract).

Summary

To extend the lifespan of Si, various materials and device structures are constantly introduced. As material property enhancement techniques, combinations of Si/Ge, Ge/Si, $Si_{1-x}Ge_x$/Si are frequently introduced in the device fabrication process to meet various physical property requirements of materials for advanced application-specific devices. Heteroepitaxy, condensation and annealing processes are commonly used in advanced device manufacturing. A small variation in composition, strain and crystallinity can result in reduced device performance or failure. The composition, structure, strain and crystallinity must be carefully monitored and controlled throughout the manufacturing process.

In this study, we have investigated a multiwavelength Raman characterization technique for detecting and monitoring Ge and Si intermixing in epitaxially grown Ge/Si after successive thermal anneals. We have demonstrated successful detection of Ge and Si intermixing after annealing under various temperatures. Very strong excitation wavelength and film structure dependence of signal-to-noise (S/N) ratio of Raman measurements was observed.

Appropriate Raman excitation wavelength selection guidelines for Ge, Si-Ge and Si material systems are given based on optical properties of materials. Examples of suitable excitation wavelength selection for properly detecting and characterizing Si and Ge intermixing were given based on the stacking order of epitaxial films and thicknesses.

References

1. B. G. Streetman and S. Banerjee, *Solid State Electronic Devices*, 6th Ed., Prentice Hall, Upper Saddle River, N.J. (2006).
2. M. Horn-von Hoegen, *Surface Science*, **537**, 1 (2003).
3. R. People and J. C. Bean, *Appl. Phys. Lett.*, **47**, 322 (1998).
4. M. Ichimura, A. Usami, A. Wakahara and A. Sasaki, *J. Appl. Phys.*, **77**, 5144 (1995).
5. F. K. LeGoues, B. S. Meyerson and J. F. Morar, *Phys. Rev. Lett.*, **66**, 2903 (1991).
6. E. A. Fitzgerald, Y. H. Xie, M. L. Green, D. Brasen, A. R. Kortan, J. Michel, Y. J. Mii and B. E. Weir, *Appl. Phys. Lett.*, **59**, 811 (1991).
7. M. Copel, M. C. Reuter, E. Kaxiras, R. M. Tromp, *Phys. Rev. Lett.*, **63**, 632 (1989).
8. J. L. Liu, C. D. Moore, G. D. U'Ren, Y. H. Luo, Y. Lu, G. Jin, S. G. Thomas, M. S. Goorsky and K. L. Wang, *Appl. Phys. Lett.*, **75**, 1586 (1999).
9. J. L. Liu, S. Tong, Y. H. Luo, J. Wan and K. L. Wang, *Appl. Phys. Lett.*, **79**, 3431 (2001).
10. B. Ackland, C. Rafferty, C. King, I. Aberg, J. O'Neill, T. Sriram, A. Lattes, C. Godek and S. Pappas, International Image Sensor Workshop, Bergen, Norway, June 2009, Session 07.
11. J. Wang and S. Lee, *Sensors*, **11**, 696 (2011).
12. S. Fama, L. Colace, G. Masini, G. Assanto and H. C. Luan, *Appl. Phys. Lett.*, **81**, 586 (2002).
13. N. Sugiyama, T. Tezuka, T. Mizuno, M. Suzuki, Y. Ishikawa, N. Shibata and S. Takagi, *J. Appl. Phys.*, **95**, 4007 (2004).

Downloaded on 2015-02-01 to IP 155.69.4.4 address. Redistribution subject to ECS terms of use (see ecsdl.org/site/terms_use) unless CC License in place (see abstract).

14. J. R. Damlencourt, B. Vincent, P. Rivallin, P. Holliger, D. Rouchon, E. Nolot, C. Licitra, Y Morand, L. Clavelier and T. Billon, *Third International SiGe Technology and Device Meeting (ISTDM 2006)*, Princeton, N.J., 1 (2006).
15. Y. H. Tan and C. S. Tan, *Thin Solid Films*, **520**, 2711 (2012).
16. A. Malik, M. Muneeb, Y. Shimura, J. Van Campenhout, R. Loo and G. Roelkens, *IEEE Photonics Technology Letters*, **25**(18), 1805 (2013).
17. H. C. Luan, D. R. Lim, L. Colace, G. Masini, G. Assanto, K. Wada and L. C. Kimerling. *MRS Proceedings*, **607**, 279 (1999).
18. H. C. Luan, D. R. Lim, K. K. Lee, K. M. Chen, J. G. Sandland, K. Wada, and L. C. Kimerling, *Appl. Phys. Lett.*, **75**, 2909 (1999).
19. L. Colace, G. Masini, G. Assanto, H. C. Luan, K. Wada and L. C. Kimerling, *Appl. Phys. Lett.*, **76**, 1231 (2000).
20. J. M. Zhang, M. Geihler, A. Göbel, T. Ruf and M. Cardona, E. E. Haller and K. Ito, *Phys. Rev. B*, **57**, 1348 (1998).
21. W. S. Yoo, K. Kang, T. Ueda and T. Ishigaki, *Appl. Phys. Exp.*, **2**, 116502 (2009).
22. F. Widulle, T. Ruf, A. Göbel, I. Silier, E. Schönherr, M. Cardona, J. Camacho, A. Cantarero, W. Kriegseis and V. I. Ozhogin, *Physca B*, **263-264**, 381 (1999).
23. M. I. Alonso and K. Winer, *Phys. Rev. B*, **39**, 10056 (1989).
24. S. Rath, M. L. Hsieh, P. Etchegoin and R. A. Stradling, *Semiconduct. Sci. Technol.*, **18**, 566 (2003).
25. C. W. Chang, M. H. Hong, W. F. Lee, K. C. Lee, S. M. Yang, M. S. Tsai, Y. Chuang, Y. T. Fan, N. Hasuike, H. Harima, T. Ueda, T. Ishigaki, K. Kang and W. S. Yoo, *AIP Advances*, **2**, 022117 (2012).
26. R. L. Aggarwal, L. W. Farrar, S. K. Saikin, A. Aspuru-Guzik, M. Stopa and D. L. Polla, *Solid State Communications*, **151**, 553 (2011).
27. T. Arguirov, M. Kittler and N. V. Abrosimov, *J. Phys.: Conference Ser.*, **281**, 012021 (2011).
28. S. K. Jang Jian, C. C Jeng, T. C. Wang, C. M. Huang, Y. L. Wang and W. S. Yoo, *J. Materials Research*, **28 (9)**, 1269 (2013).
29. *Handbook of Optical Constants of Solids III,* E. D. Palik, Editor, Academic Press, San Diego (1998).
30. http://www.cleanroom.byu.edu/OpticalCalc.phtml
31. Y. Darma, H. Murakami and S. Miyazaki, *Applied Surface Science*, **224**, 156 (2004).
32. M. H. Hong, C. W. Chang, D. C. Perng, K. C. Lee, S. K. Jang Jian, W. F. Lee, Y. Chuang, Y. T. Fan and W. S. Yoo, *AIP Advances*, **2**, 032150 (2012)

Downloaded on 2015-02-01 to IP 155.69.4.4 address. Redistribution subject to ECS terms of use (see ecsdl.org/site/terms_use) unless CC License in place (see abstract).